

# Longest excursion of fractional Brownian motion: Numerical evidence of non-Markovian effects

Reinaldo García-García,<sup>1</sup> Alberto Rosso,<sup>2</sup> and Grégory Schehr<sup>3</sup>

<sup>1</sup>Centro Atómico Bariloche, 8400 S. C. de Bariloche, Argentina

<sup>2</sup>Laboratoire de Physique Théorique et Modèles Statistiques (UMR du CNRS 8626), Université de Paris-Sud, 91405 Orsay Cedex, France

<sup>3</sup>Laboratoire de Physique Théorique (UMR du CNRS 8627), Université de Paris-Sud, 91405 Orsay Cedex, France

(Received 13 November 2009; published 13 January 2010)

We study, using exact numerical simulations, the statistics of the longest excursion  $l_{\max}(t)$  up to time  $t$  for the fractional Brownian motion with Hurst exponent  $0 < H < 1$ . We show that in the large  $t$  limit,  $\langle l_{\max}(t) \rangle \propto Q_\infty t$ , where  $Q_\infty = Q_\infty(H)$  depends continuously on  $H$ . These results are compared with exact analytical results for a renewal process with an associated persistence exponent  $\theta = 1 - H$ . This comparison shows that  $Q_\infty(H)$  carries the clear signature of non-Markovian effects for  $H \neq 1/2$ . The preasymptotic behavior of  $\langle l_{\max}(t) \rangle$  is also discussed.

DOI: 10.1103/PhysRevE.81.010102

PACS number(s): 05.40.-a, 02.50.-r, 05.70.Ln

In the last few years, there has been a growing interest in the study of *anomalous dynamics* [1,2], where by contrast with Brownian motion (BM), long-range temporal correlations induce nonstandard dynamical behaviors. Instead of diffusive behavior, anomalous dynamics typically displays a nonlinear growth of the mean-square displacement  $\langle x^2(t) \rangle \propto t^{2H}$ , where  $H \neq 1/2$  is the Hurst exponent. Such behaviors have been observed in various experimental situations including polymer networks [3], intracellular transport [4], two-dimensional rotating flows [5], or porous glasses [6]. To describe theoretically such situations, various stochastic processes have been proposed and studied. Among them, the fractional Brownian motion (fBm), initially introduced by Mandelbrot and van Ness [7], is currently playing an increasing role. For instance, the fBm was recently proposed to model the stochastic dynamics of a polymer passing through a pore (translocation) [8,9].

The fBm  $x(t)$  is a Gaussian stochastic process characterized by the following two-time correlations:

$$\langle x(t_1)x(t_2) \rangle = C(t_1, t_2) = t_1^{2H} + t_2^{2H} - |t_1 - t_2|^{2H}. \quad (1)$$

This implies that the incremental correlation function is stationary, i.e.,  $\langle [x(t_1) - x(t_2)]^2 \rangle = 2|t_1 - t_2|^{2H}$ . For  $H=1/2$ , the process  $x(t)$  is just BM. For  $H < 1/2$  the dynamics is subdiffusive, while it is superdiffusive for  $H > 1/2$ . For  $0 < H < 1$ , fBm is a nonsmooth process, i.e., it has an infinite density of zero crossings. A relevant quantity characterizing these zero crossings is the distribution  $\rho(\tau)$  of the time intervals between consecutive zeros. In many cases, which are relevant in statistical physics, this distribution has a power-law tail  $\rho(\tau) \propto \tau^{-1-\theta}$ , with  $\theta$  as the persistence exponent [10,11]. A remarkable result for processes, Gaussian or non-Gaussian, obeying Eq. (1) is the *exact* relation  $\theta = 1 - H$  [12–14]. Such processes (1) appear naturally in various interesting models of statistical physics. For instance, the fBm with  $H=1/4$  arises as a scaling limit of a tagged particle in a one-dimensional symmetric exclusion process [15]. It also describes the equilibrium temporal fluctuations of the height field of a  $d$ -dimensional Edwards-Wilkinson interface, and in that case  $H=(1-d/2)/2$  [13]. Another example where such a process as in Eq. (1), albeit non-Gaussian, appears is the

Matheron-de Marsily model of hydrodynamic flows in porous media. There it describes the longitudinal position of a particle in a  $(d+1)$ -dimensional layered random velocity field and in that case  $H=\max(1-d/4, 1/2)$  [16].

For  $H \neq 1/2$ , fBm is a non-Markovian process [7]. However the zero-crossing properties of the fBm which have been investigated up to now have not convincingly shown the signatures of these memory effects. For instance, assuming that the intervals between crossings are independent and identically distributed (renewal process) yields the correct behavior for the tail of the distribution  $\rho(\tau)$  with  $\theta = 1 - H$  [17]. More recently, on the basis of a numerical computation of the correlation function of the intervals between successive zeros, the authors of Ref. [18] claimed that the zero-crossing properties of fBm are actually described by a renewal process, which contradicts our theoretical understanding of this process [7,13]. One goal of the present Rapid Communication is thus to exhibit a property of the fBm which instead shows that temporal correlations clearly affect the zero-crossing properties of this process.

To this purpose, following a recent work [19], we study here the statistics of the longest excursion up to time  $t$ , denoted  $l_{\max}(t)$ . For a typical realization of the fBm  $x(t)$  with  $N=N(t)$  zeros in the *fixed* time interval  $[0, t]$  (see Fig. 1) let  $\{\tau_1, \tau_2, \dots, \tau_N\}$  denote the interval lengths between suc-

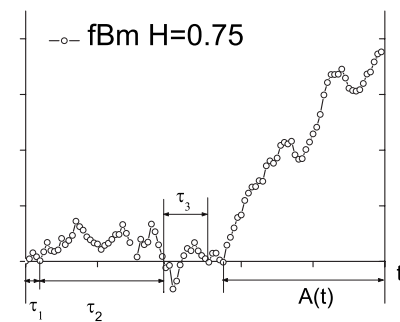


FIG. 1. Intervals between zero crossings (excursions) for the fBm in the particular case  $H=0.75$ , which was generated numerically using the Levinson algorithm. The longest excursion  $l_{\max}(t)$ , studied in this Rapid Communication, is defined in Eq. (2).

sive zeros and let  $A(t)$  denote the length (or age) of the last *unfinished* excursion. Note that with fBm being a nonsmooth process, we only consider excursions  $\tau_i$ 's larger than some cutoff  $\tau_\epsilon$ . The *extreme* observable we focus on is the length of the *longest* excursion up to  $t$ ,

$$l_{\max}(t) = \max[\tau_1, \tau_2, \dots, \tau_N, A(t)]. \quad (2)$$

We show here that the average  $\langle l_{\max}(t) \rangle$  is a quantity sensitive to the non-Markovian character of fBm. In Ref. [19], it was shown that  $\langle l_{\max}(t) \rangle$  can be conveniently computed using the exact relation

$$d\langle l_{\max}(t) \rangle / dt = Q(t), \quad (3)$$

where  $Q(t)$  is the probability that the last unfinished excursion,  $A(t)$  in Fig. 1, is the longest one,

$$Q(t) = \text{Prob}[l_{\max}(t) = A(t)]. \quad (4)$$

It was then shown that for a renewal process characterized by a persistence exponent  $\theta < 1$ , one has the exact result [19]

$$\lim_{t \rightarrow \infty} Q(t) = Q_\infty^R, \quad (5)$$

$$Q_\infty^R \equiv Q_\infty^R(\theta) = \int_0^\infty \frac{dx}{1 + x^\theta e^x \int_0^x dy y^{-\theta} e^{-y}},$$

where the superscript “ $R$ ” refers to renewal process. In this Rapid Communication, we compute numerically  $Q(t)$  (4) for fBm defined as in Eq. (1) for different values of  $0 < H < 1$ . We show that, in all these cases,  $Q(t) \rightarrow Q_\infty$  for large time  $t$ , as predicted in Ref. [19] for nonsmooth processes with  $0 < \theta < 1$ , which is the case for fBm with  $0 < H < 1$ . We then extract precisely the asymptotic value  $Q_\infty \equiv Q_\infty(H)$ : any deviation from the value  $Q_\infty^R(\theta=1-H)$  in Eq. (5) can thus be identified as a signature of non-Markovian effects.

For the purpose of numerical simulations we need to discretize the fBm path into a set of Gaussian numbers correlated through Eq. (1). Generating a sequence  $x = \{x_1, \dots, x_i, \dots, x_T\}$  of Gaussian numbers with prescribed correlations  $\langle x_i x_j \rangle = C_{i,j}$  is a two-step procedure: (i) it is first necessary to compute the matrix  $A$ , the square root of the correlation  $C$ , and (ii) each discrete path is then given by  $x = A\xi$ , where  $\xi = \{\xi_1, \xi_2, \dots, \xi_T\}$  is an uncorrelated normally distributed set of random variables. It is easy to check that paths obtained from this procedure have the required correlation matrix,

$$\langle x_i x_j \rangle = \sum_{k_1, k_2=1}^T A_{i,k_1} A_{k_2,j} \langle \xi_{k_1} \xi_{k_2} \rangle = A_{i,j}^2 = C_{i,j}. \quad (6)$$

Compared to the standard Brownian motion, building a fBm is numerically cumbersome and various algorithms have been proposed [20]. The Brownian motion has a linear cost in  $T$  and is easy to simulate paths of size  $T \sim 10^6$ . For fBm, the first step involves the full diagonalization of matrix  $C_{i,j}$  and limits to  $T \sim 1000$  the size of the path. The second step is faster and the matrix-vector product needs  $T^2$  operations. A better performance can be obtained for fBm thanks to the stationarity of the incremental correlation function. The increments  $\delta_i = x_{i+1} - x_i$  are correlated according to a Toeplitz

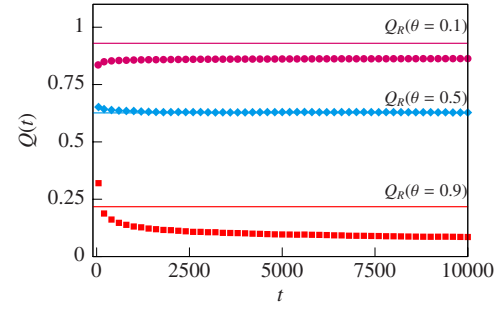


FIG. 2. (Color online)  $Q(t)$  as a function of  $t$  for  $H=0.1, 0.5$ , and  $0.9$ . The straight lines correspond to the value of  $Q_\infty^R(1-H)$  for a renewal process given in Eq. (5). This clearly illustrates that the fBm is not a renewal process.

matrix. For Toeplitz matrices special numerical methods allow us to build paths without going through the full diagonalization of  $C$ . Here, we use the Levinson algorithm, which is not the fastest algorithm but is exact for any value of  $T$  (for a practical implementation, see [21]). In this Rapid Communication we show the results obtained for fBm of size  $T=10\,000$ .

We now discuss our results for  $Q(t)$  defined in Eq. (4), which was computed by averaging over  $10^6$  samples. In Fig. 2 we show a plot of  $Q(t)$  as a function of  $t$  for different values of  $H=0.1, 0.5$ , and  $0.9$ . In all these cases our numerical data are consistent with an asymptotic behavior

$$\lim_{t \rightarrow \infty} Q(t) = Q_\infty \equiv Q_\infty(H). \quad (7)$$

We also notice that this asymptotic value is approached from above for  $H=0.1$  and  $0.5$  and from below for  $H=0.9$ . In this same figure (Fig. 2) we also plot, with dotted lines, the value of  $Q_\infty^R$  for a renewal process given in Eq. (5) with  $\theta=1-H$ . These two values  $Q_\infty$  and  $Q_\infty^R$  are clearly different as  $H$  deviates significantly from  $1/2$ . We have also checked that, for all these values of  $H$ , the persistence probability  $p_0(t) \sim t^{-1+H}$  displays a well-developed power-law behavior for  $t \geq 1000$ , so that a comparison with  $Q_\infty^R(\theta=1-H)$  is meaningful. Therefore, we can conclude safely that  $Q_\infty$  carries the signature of memory effects of the fBm for  $H \neq 1/2$ .

Although the curves for  $Q(t)$  shown in Fig. 2 indicate an asymptotic behavior as in Eq. (7) with a value for  $Q_\infty(H)$  different from  $Q_\infty^R(1-H)$ , a precise estimate of this asymptotic value  $Q_\infty(H)$  requires more effort. The time dependence of  $Q(t)$  is due to the discretization of the paths and this can be understood by studying the case of BM. It is well known that the density of zero crossings of BM is infinite: this means that, if the BM crosses zero once, it will recross zero infinitely many times immediately after the first crossing. Therefore, a proper definition of the excursions requires a regularization procedure. A convenient way to implement it is to impose that the maximal distance from the origin during an excursion should be bigger than  $x_0$ , where  $x_0$  plays the role of a spatial cutoff. To compute the finite time behavior of  $Q(t)$  we recall that the probability  $p_0(t, x_0)$  that a BM

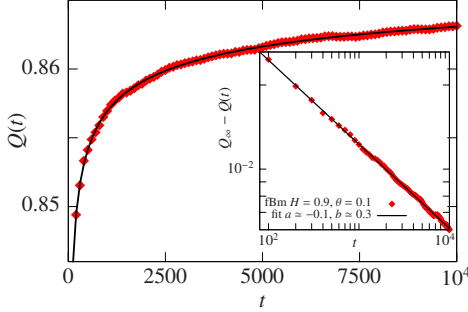


FIG. 3. (Color online) Plot of  $Q(t)$  as a function of  $t$  on a linear-linear scale for  $H=0.9$ . The solid line indicates the fit as in Eq. (13) with  $a(0.9)\approx-0.1$  and  $b(0.9)\approx 0.3$ . Inset: plot of  $Q_\infty(H=0.9)-Q(t)$  (same data as in the main figure) as a function of  $t$  in a log-log plot. The solid line corresponds to  $-a(0.9)t^{-b(H)}$ : this suggests a good quality of the fitting procedure in Eq. (13).

starting from  $x_0$  at  $t=0$  remains positive up to time  $t$  (persistence probability) is given by

$$p_0(t, x_0) \equiv p_0\left(\frac{t}{x_0^2}\right) = \text{Erf}\left(\frac{x_0}{\sqrt{2}t}\right) = \sqrt{\frac{2x_0^2}{\pi t}} + \mathcal{O}\left(\frac{x_0^2}{t^{3/2}}\right). \quad (8)$$

Following the derivation of Ref. [19] we can compute the Laplace transform  $\hat{Q}(s)$  of  $Q(t)$  in the limit  $x_0^2 \ll t$  [23],

$$\hat{Q}(s) = \frac{1}{s} \int_0^\infty dx \frac{p_0(x/s)e^{-x}}{p_0(x/s)e^{-x} + \int_0^x dy p_0(y/s)e^{-y}}. \quad (9)$$

For small  $s$ , it was shown in Ref. [19] that  $\hat{Q}(s) \sim Q_\infty^R(1/2)/s$ , where  $Q_\infty^R(1/2)=0.626\,508\dots$  [22]. To understand the effects of the discretization, one needs to compute the first correction to this leading  $1/s$  behavior when  $s \rightarrow 0$ . This has to be done carefully because a naive expansion of the persistence probability  $p_0(y/s)$  beyond the leading order as suggested by Eq. (8) in the denominator of Eq. (9) yields a diverging integral over  $y$ . Handling this singular behavior with care yields

$$\hat{Q}(s) = \frac{Q_\infty^R(1/2)}{s} + \tilde{a} \frac{x_0}{\sqrt{s}} + \mathcal{O}(1), \quad (10)$$

where  $\tilde{a}$  is given by

$$\tilde{a} = \int_0^\infty \frac{e^{-x} x^{1/2}}{[x^{-1/2} e^{-x} + \sqrt{\pi} \text{Erf}(\sqrt{x})]^2} dx = 0.23970\dots \quad (11)$$

Going back to real time this yields finally

$$Q(t) = Q_\infty^R(1/2) + \tilde{a} \sqrt{x_0^2/t} + \mathcal{O}(x_0^2/t). \quad (12)$$

Motivated by this result for Brownian motion (12), we propose to describe the data for  $Q(t)$  in Fig. 2 by

$$Q(t) \sim Q_\infty(H) + a(H)t^{-b(H)}. \quad (13)$$

In particular, from Eq. (12), one expects  $b(1/2)=1/2$ . We have checked that this form (13) describes very well our data for  $Q(t)$  for all the values of  $0 < H < 1$  that we have studied.

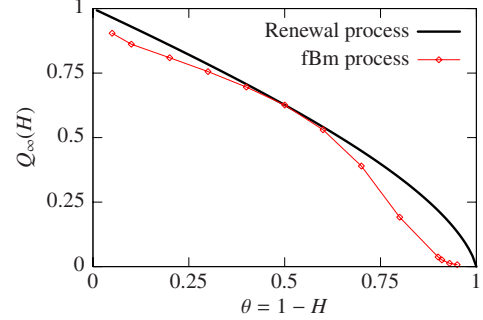


FIG. 4. (Color online) The symbols indicate the numerical estimate of  $Q_\infty(\theta=1-H)$ , extracted from the fitting procedure in Eq. (13). For comparison, we have also plotted  $Q_\infty^R(\theta=1-H)$  for a renewal process (5). This plot clearly shows that, except for  $H=1/2$ , the fBm is not a renewal process.

In the inset of Fig. 3, we show a plot of  $Q(t) - Q_\infty(H=0.9)$  as a function of  $t$  on a log-log scale, while the main figure shows a plot of  $Q(t)$  as a function of  $t$  on a linear-linear plot. This fitting procedure (13) hence provides a reliable way to estimate the asymptotic value  $Q_\infty(H)$ . In Fig. 4 we have plotted these values as functions of  $\theta=1-H$ . For comparison, we have also plotted the values of  $Q_\infty^R(\theta)$  for the renewal process (5): these two curves are clearly different (except for  $H=1/2$ , which corresponds to Brownian motion).

In Fig. 5, we show our numerical data for  $a(H)$  and  $b(H)$ . These indicate that the exponent  $b(H)$  exhibits a maximum for  $H \sim 0.5$ , where  $b(1/2)=1/2$ . On the other hand, one finds that  $b(H) \rightarrow 0$  for  $H \rightarrow 0$  and  $H \rightarrow 1$ ; therefore, it becomes very difficult to extract a reliable value for  $\theta$  close to 0 and 1. For  $H=1$ , the fBm is simply a linear function of time  $t$ ,  $x(t)=\zeta t$ , where  $\zeta$  is a Gaussian random variable of unit variance. It is thus easy to see that  $Q_\infty=1$  in that case. Although it is very difficult to extract a reliable value of  $Q_\infty(H)$  for  $H>0.95$ , one expects that  $Q_\infty(H) \rightarrow 1$ , smoothly, when  $H \rightarrow 1$ . Similarly, our data suggest that  $Q_\infty(H)$  vanishes smoothly as  $H \rightarrow 0$ . Finally, we notice that  $a(H)$  changes sign for  $H \sim 0.7$ : it is positive for  $H \geq 0.7$  and negative for  $H \leq 0.7$ .

To conclude, we have presented a numerical computation of the mean longest excursion  $\langle l_{\max}(t) \rangle$  for the fBm with Hurst index  $0 < H < 1$ . We have shown that  $\langle l_{\max}(t) \rangle \sim Q_\infty(H)t$  for large  $t$ , where  $Q_\infty(H)$  is an interesting feature

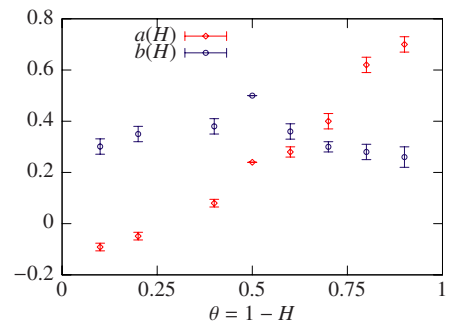


FIG. 5. (Color online) Plot of  $a(H)$  and  $b(H)$  as functions of  $H=1-\theta$ .

of fBm. We have also demonstrated that this quantity is very sensitive to temporal correlations characterizing this process. Therefore, at variance with the recent claim of Ref. [18], our numerical results clearly show that the zero crossings of fBm cannot be described by a renewal process. We point out that the quantity studied here is sensitive to the full joint distribution of the time intervals between crossings, while the numerical work presented in Ref. [18] only studied the correlation function between two such intervals. Finally, we hope that the nontrivial dependence of  $Q_\infty(H)$  as well as  $a(H)$  and

$b(H)$  shown in Figs. 4 and 5 will stimulate further analytical progress on the study of fBm.

This work was supported by the France-Argentina MINCYT-ECOS Contract No. A08E03. We thank Joachim Krug for pointing out Ref. [18]. We acknowledge C. Godrèche and S. N. Majumdar for stimulating discussions at the earliest stage of this work. R.G.G. acknowledges support from CONICET and the hospitality at LPT and LPTMS in Orsay.

- 
- [1] J.-P. Bouchaud and A. Georges, Phys. Rep. **195**, 127 (1990).
  - [2] R. Metzler and J. Klafter, Phys. Rep. **339**, 1 (2000).
  - [3] F. Amblard, A. C. Maggs, B. Yurke, A. N. Pargellis, and S. Leibler, Phys. Rev. Lett. **77**, 4470 (1996).
  - [4] A. Caspi, R. Granek, and M. Elbaum, Phys. Rev. Lett. **85**, 5655 (2000).
  - [5] T. H. Solomon, E. R. Weeks, and H. L. Swinney, Phys. Rev. Lett. **71**, 3975 (1993).
  - [6] S. Stapf, R. Kimmich, and R.-O. Seitter, Phys. Rev. Lett. **75**, 2855 (1995).
  - [7] B. B. Mandelbrot and J. W. van Ness, SIAM Rev. **10**, 422 (1968).
  - [8] Y. Kantor and M. Kardar, Phys. Rev. E **69**, 021806 (2004).
  - [9] A. Zoia, A. Rosso, and S. N. Majumdar, Phys. Rev. Lett. **102**, 120602 (2009).
  - [10] B. Derrida, A. J. Bray, and C. Godrèche, J. Phys. A **27**, L357 (1994); A. J. Bray, B. Derrida, and C. Godrèche, EPL **27**, 175 (1994).
  - [11] For a review, see S. N. Majumdar, Curr. Sci. **77**, 370 (1999).
  - [12] A. Hansen, T. Engoy, and K. J. Maloy, Fractals **2**, 527 (1994); S. Maslov, M. Paczuski, and P. Bak, Phys. Rev. Lett. **73**, 2162 (1994); M. Ding and W. Yang, Phys. Rev. E **52**, 207 (1995).
  - [13] J. Krug *et al.*, Phys. Rev. E **56**, 2702 (1997).
  - [14] M. Constantin, C. Dasgupta, P. Punyindu Chatraphorn, S. N. Majumdar, and S. Das Sarma, Phys. Rev. E **69**, 061608 (2004).
  - [15] R. Arratia, Ann. Probab. **11**, 362 (1983).
  - [16] S. N. Majumdar, Phys. Rev. E **68**, 050101(R) (2003).
  - [17] J. Krug and H. T. Dobbs, Phys. Rev. Lett. **76**, 4096 (1996).
  - [18] R. Cakir, P. Grigolini, and A. A. Krokhin, Phys. Rev. E **74**, 021108 (2006).
  - [19] C. Godrèche, S. N. Majumdar, and G. Schehr, Phys. Rev. Lett. **102**, 240602 (2009).
  - [20] C. Monthus and T. Garel, e-print arXiv:0910.0111, and references therein.
  - [21] T. Dieker, Master thesis, Vrije Universiteit Amsterdam, 2002; <http://www2.isye.gatech.edu/adieker3>
  - [22] J. Pitman and M. Yor, Ann. Probab. **25**, 855 (1997).
  - [23] This formula is valid up to terms of order  $\mathcal{O}(x_0^2/t)$ . The precise evaluation of these terms goes beyond the scope of this Rapid Communication.